# DIRECTED SIDEWARD FLOW OF FRAGMENTS AND SECONDARY PARTICLES IN RELATIVISTIC HEAVY ION COLLISIONS*

C.H. PINKENBURG AND K.D. HILDENBRAND

FOPI COLLABORATION**

Gesellschaft für Schwerionenforschung, GSI, Darmstadt, Germany

*(Received December 8, 1995)*

In experiments at the SIS facility at GSI Darmstadt systematic studies of the directed sideward flow in central and semi-central heavy ion collisions have been performed. The symmetric systems Ni + Ni and Au + Au were investigated at energies between 100 and 2000 $A$MeV with FOPI, a $4\pi$ detection system for charged particles. For the first time the flow patterns, represented by the in-plane transverse momentum per nucleon or the azimuthal emission distribution at midrapidity have been investigated for intermediate mass fragments ($Z \geq 3$) as well as for the secondary products $\pi^+$, $\pi^-$, $K^+$, $K^0_s$, and $\Lambda$-particles. As known from many earlier studies the fragments show a clear flow signal, stronger than that of the light charged particles or nucleons. Both $\pi^+$ and $\pi^-$ display an almost vanishing signal. The same is true for the strange products $K^+$ and $K^0$ whereas the $\Lambda$-particles, co-produced with the $K^+$, show a distribution very similar to the proton signal.

PACS numbers: 25.70.Pq

## 1. Introduction

Among the outstanding results of the exclusive investigation of heavy ion reactions at relativistic energies are the collective features which manifest themselves in a common, coherent movement of products after the

* Presented at the XXIV Mazurian Lakes School of Physics, Piaski, Poland, August 23–September 2, 1995.

** The FOPI Collaboration comprises members from the following institutions at present: IPNE Bucharest, KFKI Budapest, LPC Clermont-Ferrand, GSI Darmstadt, FZ Rossendorf, Univ. Heidelberg, ITEP Moscow, Kurchatov Inst. Moscow, CRN Strasbourg, Univ. Warsaw, RBI Zagreb.

collision, the "flow" of nuclear matter. Signatures such as the "side-splash" (directed sideward or transverse flow [1]) or the "squeeze-out" [2] observed in semi-central collisions in the reaction plane and perpendicular to it, respectively, have been known since the first experiments about a decade ago. More recently a radial collective expansion has been established in highly-central collisions, too [3, 4]. The early euphoria that the analysis of these findings might lead right away to a determination of the quantities governing the nuclear equation of state has made room for the insight that *e.g.* the magnitude of the directed sideward flow is not just determined by effects of compression/decompression but rather by a variety of phenomena leading to ambiguities in the choice of the needed parameters (see *e.g.* [3] and references therein). That is why only exclusive studies of many systems at various energies looking at as many products and/or observables as possible and their confrontation with state-of-the-art theories will help to get further in our understanding of the behaviour of the hot and compressed nuclear matter formed in these collisions.

At GSI during the past years we have undertaken systematic studies of light and heavy symmetric collision systems, varying the bombarding energies over the whole SIS energy range up to 2000 $A$MeV. In this contribution we present a first comparison of the directed sideward flow for a variety of ejectiles, ranging from light charged particles and clusters over charged pions to the strange products $K^+$, $K^0_s$ and $\Lambda$-particles. These probes are typical representatives of different incident energy regimes: clusters prevail at low energies up to a few hundred $A$MeV; pions are produced in increasing number once their free production threshold (290 $A$MeV) is surpassed. $K^+$ (and $K^0_s$), coproduced with a $\Lambda$ in the same nucleon-nucleon collision, have a $N + N$ threshold near 1580 $A$MeV; hence our first experiment at SIS to look for strange particles used the highest available beam energy. The production of $K^-$ is still strongly suppressed at this energy, since its threshold lies at about 2500 $A$MeV (of course all products can also be produced below the free threshold in nucleon–nucleon collisions, at very reduced rates). The different flow characteristics as observed for these ejectiles may tell us not only about their production in high-energetic collisions, but especially about their interaction with the surrounding hot matter.

## 2. Experimental details

The results described here have been obtained in various experiments during the completion phase of the FOPI detection system. The cluster (IMF) measurements in Au + Au (incident energies 100 to 1060 $A$MeV) have been performed with the so-called phase I setup [5] which comprised a time-of-flight wall covering the full azimuth of the lab-angles 1.2° to 30°. It

consists out of 764 scintillators measuring the deposited energy $\Delta E$ and the time of flight ToF; both quantities together deliver the charge of the products. For heavier/slow ejectiles which are stopped in the scintillators the $\Delta E$ information is delivered by a shell of 128 transmission ionization chambers or, at smaller angles, by 60 thin scintillator paddles placed in front of the main wall.

The new $\pi$, $K$ and $\Lambda$ data presented here (systems Au + Au at 1060 $A$MeV and Ni + Ni at 1930 $A$MeV, respectively) have been taken with the almost finished detector setup, including the Central Drift Chamber (CDC), housed in the 0.6 T field of a solenoid magnet; this cylindrical chamber in the inner bore of which the target is placed identifies products over the full azimuth between $\theta_{\mathrm{lab}} = 30° - 150°$ by measuring the specific energy loss $\Delta E$ and the momentum (via $B\rho$ analysis). It is surrounded by a barrel of 180 scintillator strips aligned parallel to the beam axis. ToF and the momentum measurement are used for an additional mass determination [6]; this redundant information helps to identify the rare kaons in presence of the pions and protons which are by orders-of-magnitude more abundant [7]. At the time of the present experiments only one third of the barrel scintillators had been installed. In the meanwhile (fall 1995) the full FOPI system is operational, including the second drift chamber for the forward angular range down to $\theta_{\mathrm{lab}} = 7°$, hence allowing momentum and mass determination over a dominant part of the phase space.

The detection of the neutral products ($K^0_s$ and $\Lambda$) is possible via their decay into $(\pi^+,\pi^-)$ and $(p,\pi^-)$ pairs, respectively. One searches for such pairs of potential decay products which originate from a secondary decay vertex; this vertex is required to be shifted transversally by more than 1.2 cm ($K^0_s$) or 2.0 cm ($\Lambda$) from the primary event vertex. The spectra of the invariant masses calculated with candidate pairs show clear peaks at the respective particle masses on top of a combinatorial background. Details of the procedure can be found in [7].

The determination of the impact parameter of a collision and hence the centrality of the considered event is a key issue in the analyses. The most frequently used criterion is the charged particle multiplicity, PM, of the event [1], sometimes restricted to 'participating' products by excluding certain rapidity intervals or pions [8]. In the analyses described in the following we have adopted the first definition; the plateau-like experimental distributions with a fall-off at high multiplicities are cut into 5 equally wide bins, PMi ($i$ = 1 to 5), with PM5 beginning at the value where the distribution has dropped to half the plateau value. Hence increasing numbers in i denote on the average increasing centrality of the selected events. This criterion is a decent one for investigating effects showing a smooth trend when going from peripheral to more central collisions as we expect in the

investigations of flow effects. One has to note, however, that in studies requiring a more stringent cut on highly central events the bare multiplicity is a poor selection criterion; it can be replaced by various other quantities [9] but even then the extrapolation of effects down towards $b = 0$ is not straightforward [3].

## 3. Cluster flow

The traditional way [8, 10] of describing the directed sideward flow calculates the average transverse momentum in the reaction plane of an event (the summed in-plane momentum components over the number of involved nucleons, $\langle P_x \rangle / A$); the plane itself is *e.g.* determined by the method of [10]. This quantity can be looked at for various bins of centrality in an integrated form or differentially as function of the rapidity. Figure 1 shows such a plot for the Au + Au reaction at 250 $A$MeV and the multiplicity bin PM4. Throughout this article we use on the rapidity axis the scaled rapidity $y^{(o)} \equiv y^{(o)}_{\rm cm} = y^{\rm cm}/y^{\rm cm}_p = (y - y^{\rm cm}_p)/y^{\rm cm}_p = y/y^{\rm cm}_p - 1$.

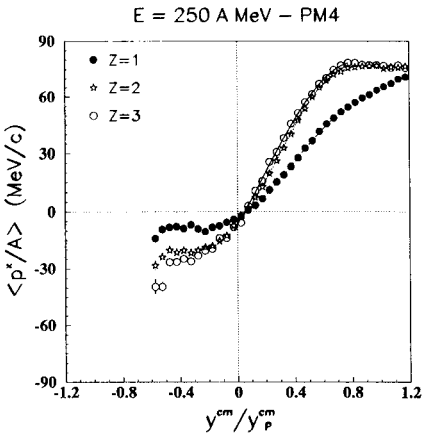


Fig. 1. Directed sideward flow of $Z = 1$, $Z = 2$ and $Z = 3$ fragments in the reaction Au + Au at 250 $A$MeV (centrality bin PM4). The curves show the typical S-shaped form and demonstrate a stronger increase at midrapidity with increasing charge (or mass) of the products. The reduced rapidity plotted on the abscissa (see text for definition) is identical to the one used in Figures 3 and 4.

The curves for $Z = 1$, $Z = 2$ and $Z = 3$ show the typical S-shaped form [8, 10] yielding a maximum flow signal in the vicinity of the beam rapidity ($y^{(o)} = 1$). In this range one finds a mixture of participant and spectator matter; therefore one often uses the "flow parameter" F, defined as the slope

of the curves at origin; a larger F signals a stronger flow. Figure 1 demonstrates that clusters show a definitely stronger effect ("clusters go with the flow"). Obviously $Z = 1$ fragments are subjected to stronger thermal effects (a complete random emission would give a zero signal); for clusters the undirected thermal velocities seem to have lower relative importance. This result of the flow increasing with the mass of the products has principally been known for a long time [11] but only with the event of the new $4\pi$ devices (FOPI and EOS, [5, 12]) systematic cluster flow measurements could be carried out. For detailed descriptions of the flow of hadrons with emphasis on clusters in Au + Au collisions at energies ranging from 100 to 800 $A$MeV we would like to refer to an upcoming paper [13].

## 4. Pionic flow in Au + Au

Although charged pions were already investigated in the first-generation experiments, results on global quantities like flow were scarce and restricted to light systems [14]. First experiments with heavy systems, Au + Au around 1 $A$GeV, revealed similar squeeze-out patterns as baryons around midrapidity (see [15] for $\pi^0$ and [16] for $\pi^+$ results). These data were only taken within a small window around midrapidity.

We have investigated the sideward flow of charged pions in the system Au + Au at 1060 $A$MeV by means of the central drift chamber, CDC, which sees about 70% of all emitted charged pions in this reaction. Because it covers the angles backwards of $\theta_{\mathrm{lab}} = 35°$ the analysis is restricted to the backward hemisphere in the c.m. system (negative c.m. rapidities). For the centrality selection we have used the multiplicity of charged particles measured in the forward wall. The bins PM3 (peripheral) and PM5 (central) correspond to average impact parameters of $6.7 \pm 0.9$ fm and $2.5 \pm 1.1$ fm. The reaction plane has been reconstructed using the prescription of [10] with a precision of $\sigma \approx 17°$ for the PM3- and $\sigma \approx 25°$ for the PM5- bin. The extracted parameters shown later are corrected for this uncertainty, the corrections being of the order of 10% to 30% for the $a_1, a_2$-parameters discussed below. For technical reasons we use a somewhat different way of deriving the directed flow in the present analysis: In Figure 2 the azimuthal distributions of protons, $\pi^-$ and $\pi^+$ are plotted for various bins in rapidity, the rapidity bins ranging from slightly positive values (denoting the forward hemisphere) to the target rapidity (located at $-1$) and beyond.

In the case of the protons all distributions are clearly structured: midrapidity distributions exhibit two bumps at 90° an 270°; when going towards target rapidity these bumps vanish in favor of a single one growing at 180°. This latter structure represents the in-plane directed flow showing up at this angle in the backward hemisphere, forward it would be located at 0°

by definition. The two side bumps reflect the squeeze-out, the well known midrapidity emission of matter perpendicular to the reaction plane.

Compared to the protons the pions show reduced, almost vanishing structures (with the $\pi^+$ being even weaker than the $\pi^-$). Because of certain inefficiencies of the CDC for pions in areas of high particle densities the distributions should be looked at only for $\phi \geq 180°$ for $\pi^-$ ($\phi \leq 180°$ for $\pi^+$); by requiring azimuthal symmetry this defect can be corrected.

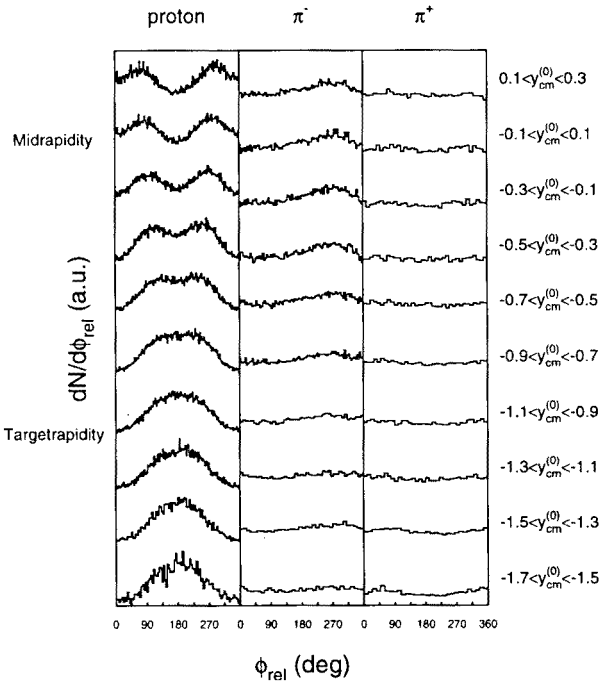


Fig. 2. Azimuthal distributions of protons, $\pi^+$ and $\pi^-$ for various cuts in rapidity; displayed are events of the centrality bins PM3.

Based on these characteristics the distributions have been fitted with the following expression:

$$\frac{dN}{d\Phi} = a_0 \left[1 + a_1 \cos(\Phi) + a_2 \cos(2\Phi)\right] ,$$

$a_1$ represents the strength of the emission into the reaction plane; a conventional sideward flow as presented in the previous chapter should show a negative value in the backward hemisphere. With $a_1 \approx 0$ a positive $a_2$ describes the emission perpendicular to the reaction plane at midrapidity. In other rapidity ranges with $a_1 \neq 0$ negative $a_2$-parameters reveal rather

the degree of focussing into the reaction plane (note that the sign of $a_2$ in the figure is reversed compared to the fit).

A quantitative comparison of the directed flow determined in this way with the method of $\langle P_x/A \rangle$ as used in chapters 3 and 5 is difficult; so we will keep the present discussion qualitatively and concentrate on the differences between the various particles. The derived values for $a_1$, $a_2$ are displayed in Figure 3 as a function of the scaled rapidity for peripheral and central collisions.

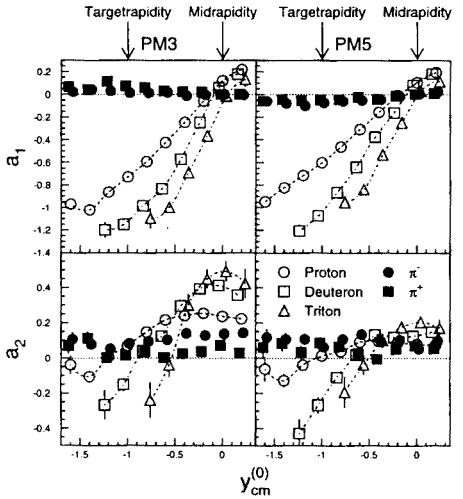


Fig. 3. Extracted flow parameters for pions and protons, deuterons and tritons as function of the scaled rapidity. Left: peripheral, right: central events (PM3 and PM5, respectively). Both kinds of charged pions are very similar in behavior, but they clearly differ from the baryons, showing much weaker signals in all representations. See text for detailed discussion.

The $a_1$-parameter for the baryons show the expected behaviour in going from negative through zero to positive with increasing rapidity; as in the case of the cluster flow the effect is more pronounced for the composite particles. At midrapidity their $a_2$ component shows the squeeze-out signature, somewhat weaker for the PM5 bin, and towards target rapidity a focussing of their in-plane flow. Note that if $a_1 \neq 0$ a large $a_2$ component signals a broader distribution of the in-plane flow. The in-plane focussing is stronger for heavier particles.

The charged pions show a completely different behavior as their flow effects are much smaller. In PM3 (peripheral collisions) the $\pi^-$ show an $a_1$ component close to zero, indicative of no preferred emission into the plane; for $\pi^+$ the slightly positive $a_1$ values even point towards an anticorrelation with the baryonic flow. The small positive $a_2$ values for both particles may

indicate a slight preference for emission perpendicular to the plane. The more central collisions (PM5 bin) show very similar results, except the $a_1$ parameters being slightly negative, denoting an in-plane emission as for the baryons but much weaker in amplitude.

The features of the pions which differ considerably from the baryon results must be connected to the propagation of the mesons inside the nuclear medium after their formation in nucleon-nucleon collisions. At our energies this formation occurs predominantly via the $\Delta(1232)$-resonance. Inside the nuclear matter each pion undergoes a couple of interactions before being released; it may be reabsorbed or scattered by the surrounding (spectator-) matter so finally only the "latest" pions are detected delivering rather a picture of the freeze-out situation than a glimpse of the early interaction. The different Coulomb forces for $\pi^+$ and $\pi^-$ may give rise to differences in some observables, too. Theoretical descriptions have to take into account all these secondary interactions in a decent way; first attempts in the framework of the IQMD-model [17] are able to reproduce the experimental trends shown here.

## 5. Flow of strange particles

For our first investigations of strangeness production we have chosen a light symmetric system, $^{58}$Ni $+^{58}$Ni at 1930 $A$MeV, the highest available SIS energy. As in the case of the pions these products were identified with the central drift chamber which restricts the analysis to the backward c.m. hemisphere. All results are shown under the requirement of $\langle P_x \rangle / m \geq 0.5$; the normalization of the momenta to the respective particle mass is used for an easier comparison of the different particle species. The influence of the various cuts and phase space limitations is discussed in [7].

Figure 4 shows the distributions of $\langle P_x \rangle / m$ as function of the scaled rapidity $y_{\mathrm{cm}}^{(o)}$ for the strange products $K^+$, $K_s^0$, and $\Lambda$ as well as for protons. Within the errors (only statistical ones are shown) the kaon distributions do not reveal any flow signal; they are compatible with isotropic emission. The $\Lambda$s, however, exhibit a pattern very similar to that of the protons, in qualitative agreement with a recent similar investigation [18].

This is a very striking result, since $K$s and $\Lambda$s are co-produced in the same nucleon–nucleon collision. The production takes place probably in the early phase of the reaction when the highest collision energies are available, whereas the flow pattern is expected to develop somewhat later during the expansion phase. By very qualitative arguments the $\Lambda$-flow can be explained by the high $\Lambda$, $p$ scattering cross section: The strange baryons are taken along by the non-strange ones with a comparable average velocity profile (in a similar way as an accelerator beam reaches the absolute velocity and

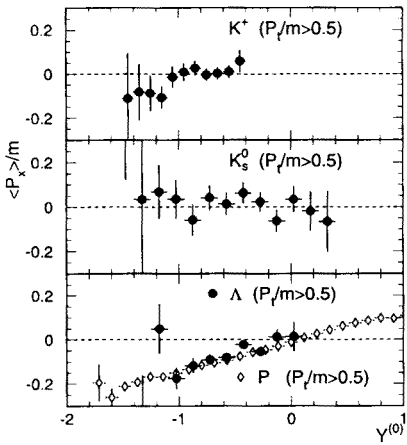


Fig. 4. Mean transverse momenta $< P_x/m >$ as function of the scaled rapidity for $K^o_s$, $K^+$, $\Lambda$, and protons (reaction $^{58}$Ni + $^{58}$Ni at 1930 $A$MeV). For the normalization of $\langle P_x \rangle$ the respective particle mass m is used. Within the error bars (statistical errors only) the two upper plots show a signal comparable to zero, *i.e.* no sideward flow, whereas the $\Lambda$s follow the proton flow (lowest plot).

the velocity spread of a parallel intense electron beam in a cooler facility). The $K^+$, $p$ scattering cross section, on the other hand, is much smaller, so the kaon final state interaction is strongly reduced (which makes positive kaons interesting objects to study). Specific flow patterns offer therefore a direct possibility to gain information on the in-medium kaon potential as demonstrated by calculations for the Au + Au and our Ni + Ni-system [19]. For a precise tuning of the potential a precision of the flow determination in terms of $\langle P_x \rangle / m$ is required which exceeds the one of the present experiment, but will hopefully be reached in upcoming runs with the completed FOPI device.

## REFERENCES

[1] H.A. Gustafsson *et al.*, *Phys. Rev. Lett.* **52**, 1590 (1984).
[2] D. L'Hôte *et al.*, *Nucl. Phys* **A488**, 457c (1988).
[3] S.C. Jeong *et al.*, *Phys. Rev. Lett.* **72**, 3468 (1994).
[4] W.C. Hsi *et al.*, *Phys. Rev. Lett.* **73**, 3367 (1994).
[5] A. Gobbi *et al.*, *Nucl. Instrum. Methods Phys. Res.* **A324**, 156 (1993).
[6] J.L. Ritman *et al.*, *Nucl. Phys. B - Proc.Suppl.* **44**, 708 (1995).
[7] J.L. Ritman *et al.*, *Z. Phys.* **A352**, 355 (1995).
[8] K.G.R. Doss *et al.*, *Phys. Rev. Lett.* **57**, 302 (1986).
[9] W. Reisdorf, Proc. XX Workshop on Gross Properties of Nuclei and Nuclear Excitation, Hirschegg, Austria, January 1992.

[10] P. Danielewicz *et al.*, *Phys. Lett.* **157B**, 146 (1985).
[11] K.H. Kampert, J. Phys. G **15**, 691 (1989).
[12] G. Rai *et al.*, *IEEE Trans. Nucl. Sci.* **37**, 56 (1990).
[13] R. Donà, F. Rami, *et al.*, to be published.
[14] D. L'Hôte *et al.*, *Nucl. Phys.* **A519**, 331c (1990).
[15] L.B. Venema *et al.*, *Phys. Rev. Lett.* **71**, 835 (1993).
[16] D. Brill *et al.*, *Phys. Rev. Lett.* **71**, 336 (1993).
[17] S. Bass, Diploma thesis, Report GSI–93–13.
[18] M. Justice *et al.*, Proceedings to Quark Matter 1995.
[19] G.Q. Li *et al.*, *Phys. Rev. Lett.* **74**, 235 (1995), and private communication.